

# Critical Fluctuations in the Microwave Complex Conductivity of BSCCO and YBCO Thin Films

D.-N. Peligrad\*, B. Nebendahl\*, and M. Mehring

2. *Physikalisches Institut, Universität Stuttgart, 70550 Stuttgart, Germany*

A. Dulčić

*Department of Physics, Faculty of Science, University of Zagreb, POB 331, 10002 Zagreb, Croatia\**

(Dated: Submitted to Phys. Rev. Lett. August 17, 2019)

Critical fluctuations above  $T_c$  are studied in the microwave complex conductivity of BSCCO-2212, BSCCO-2223, and YBCO thin films. The analysis of the experimental data yields the temperature dependences of the reduced coherence length  $\xi(T)/\xi_0$ . Two critical regimes are observed, having the static critical exponent  $\nu = 1$  close to  $T_c$ , and a crossover to  $\nu = 2/3$  at higher temperatures. In more anisotropic superconductors the reduced coherence lengths are larger, and the critical states extend to higher temperatures.

PACS numbers: 74.40.+k, 74.25.Nf, 74.76.Bz

The nature of superconducting fluctuations in high-temperature superconductors has continued to attract a great deal of attention. The small coherence lengths, high transition temperatures, and large anisotropy due to the layered structure make the fluctuations of the order parameter much stronger than in classical low temperature superconductors. Particularly intriguing has appeared the possibility of observing critical fluctuations in a fairly wide temperature range around  $T_c$ . In this regime the critical exponents deviate with respect to their mean-field values. Renormalization group theory provides an appropriate description of this phenomenon. One obtains scaling laws and universality features which are of great importance in identifying the nature of the phase transition [1]. The critical fluctuations in high- $T_c$  superconductors have been studied by penetration depth [2, 3], specific heat [4, 5], magnetization [4], resistivity [6, 7, 8], thermal expansivity [9], and two-coil inductive measurements [10]. The conclusions drawn from these data seemed to point at critical behavior belonging to the 3D XY universality class in high- $T_c$  superconductors. However, the discrepancies in the region of the critical behavior varied from a fraction of a degree [7, 8] to  $\pm 10$  K [2, 9].

Common difficulties in an analysis of the experimental data involve the subtraction of a background signal on which the fluctuation component is superimposed, and the determination of the unknown parameters by fitting procedures. In this paper we present novel results and a new type of data analysis of the microwave fluctuation conductivity in thin films of high temperature superconductors  $Bi_2Sr_2CaCu_2O_{8+\delta}$  (BSCCO-2212),  $Bi_2Sr_2Ca_2Cu_3O_{10+\delta}$  (BSCCO-2223), and  $YBa_2Cu_3O_{7-\delta}$  (YBCO). The advantage of the  $ac$  method is that one obtains two experimental data sets, i. e. the real and imaginary parts of the fluctuation conductivity, both of which have to corroborate with a given

theoretical model using the same set of parameters. It represents therefore a more stringent test on the nature of the fluctuations than the methods yielding a single experimental curve. Further advantage of the  $ac$  fluctuation conductivity is that  $T_c$  can be determined straightforwardly from the experimental data since the real part has a finite peak at  $T_c$ . This unambiguous and precise determination of  $T_c$  is very important in the analysis of the critical exponents near  $T_c$ . Utilizing these features, we achieve the main result of this paper, which is the experimentally determined temperature dependences of the coherence lengths above  $T_c$  in BSCCO and YBCO thin films. Quite surprisingly, we observe in all our samples two critical regimes with the static critical exponents  $\nu = 1$  close to  $T_c$ , and a crossover to  $\nu = 2/3$  at higher temperatures. With the increasing degree of anisotropy from YBCO to BSCCO-2212, and BSCCO-2223, we observe a systematic rise of the normalized coherence length and a consequent extension of the critical behavior to higher temperatures.

YBCO thin films having 200 nm thickness were grown on  $MgO$  substrate. BSCCO-2212 (350 nm) and BSCCO-2223 (100 nm) thin films were grown on  $LaAlO_3$  and  $NdGaO_3$  substrates, respectively. For microwave measurements the sample was cut typically to 4 mm in length, and 1 mm in width. It was mounted on a sapphire cold finger and positioned in the center of an elliptical copper cavity resonating in  $eTE_{111}$  mode at  $\approx 9.5$  GHz. The microwave electric field  $E_\omega$  was parallel to the longer side of the film sample. With this configuration, the induced microwave current was flowing only in the ab-plane of the superconducting film. The temperature of the sample could be varied from 2 K to room temperature by a heater and sensor assembly mounted on the sapphire sample holder while the microwave cavity remained in pumped helium flow at 1.7 K. The  $Q$ -factor was measured by a recently introduced modulation tech-

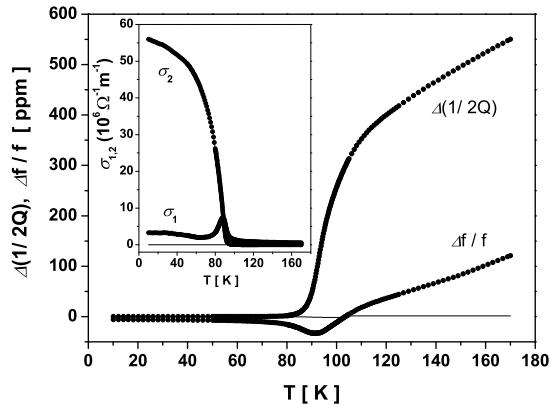


FIG. 1: Temperature dependences of the experimentally measured  $\Delta(1/2Q)$  and  $\Delta f/f$  in BSCCO-2212 thin film. The inset shows the real ( $\sigma_1$ ) and imaginary ( $\sigma_2$ ) parts of the complex conductivity.

nique [11], which enables the resolution of  $\Delta(1/2Q)$  to 0.02 ppm. The empty cavity had a value of  $1/2Q$  close to 20 ppm, which was subtracted from the data measured in the thin films. The change of the resonant frequency of the cavity loaded with the sample was monitored by a microwave frequency counter. Fig. 1 shows the experimental values of  $\Delta(1/2Q)$  and  $\Delta f/f$  for the BSCCO-2212 thin film. The complex frequency shift  $\Delta\tilde{\omega}/\omega = \Delta f/f + i\Delta(1/2Q)$  is related to the sample and cavity parameters through the cavity perturbation analysis [12]

$$\frac{\Delta\tilde{\omega}}{\omega} = \frac{\Gamma}{N} \left[ 1 - N + \frac{(\tilde{k}/k_0)^2 N}{\left[ \coth(i\tilde{k}d/2) + \tanh(i\tilde{k}\zeta) \right] i\tilde{k}d/2} \right]^{-1}, \quad (1)$$

where  $\Gamma$  is the filling factor of the sample in the cavity, and  $N$  is the depolarization factor of the film. The complex wavevector in the film is  $\tilde{k} = k_0 \sqrt{1 - i\tilde{\sigma}/(\epsilon_0\omega)}$ , where  $k_0 = \omega\sqrt{\mu_0\epsilon_0}$  is the vacuum wavevector, and  $\tilde{\sigma} = \sigma_1 - i\sigma_2$  is the complex conductivity of the film. The thickness of the film is  $d$ , and  $\zeta$  is the asymmetry parameter due to the substrate [12]. The unknown parameters in Eq. (1) have been evaluated from the ratio of the slopes of the experimental curves  $\Delta(1/2Q)$  and  $\Delta f/f$  in the normal state far above  $T_c$ , and using  $\sigma_n = 6.4 \cdot 10^5 \Omega^{-1} m^{-1}$  for the normal state conductivity at 150 K where the experimental slopes were evaluated. Eq. (1) can then be used to convert the experimental data for  $\Delta(1/2Q)$  and  $\Delta f/f$  at any temperature to obtain the corresponding experimental values of  $\sigma_1$  and  $\sigma_2$ . The results for the whole temperature range are shown in the inset to Fig. 1. Similar results for the complex conductivity in BSCCO-2212 have been obtained previously on single crystals [13].

In this paper we focus on  $\sigma_1$  and  $\sigma_2$  at, and above

$T_c$ , shown on an expanded scale in Fig. 2(a). Here the reduced temperature  $\epsilon = \ln(T/T_c)$  is used. We proceed now with the analysis of the *ac* fluctuation conductivity above  $T_c$  in terms of the recently developed expression which accounts for the effects of short wavelength cutoff in the fluctuation spectrum [14]

$$\tilde{\sigma} = \frac{e^2}{32\hbar\xi_{0c}} \left( \frac{\xi(T)}{\xi_0} \right) [\mathcal{S}_1(\omega, T, \Lambda_{ab}, \Lambda_c) + i\mathcal{S}_2(\omega, T, \Lambda_{ab}, \Lambda_c)]. \quad (2)$$

The prefactor is the Aslamazov-Larkin term for the 3D case. The normalized coherence length  $\xi(T)/\xi_0$  is the same for the in-plane and *c*-axis coherence lengths, i. e.  $(\xi_{ab}(T)/\xi_{0ab}) = (\xi_c(T)/\xi_{0c})$  [14], so that we use it without subscripts. The  $\mathcal{S}$ -functions contain the frequency and temperature dependence as well as the cutoff effects through the dimensionless parameters  $\Lambda_{ab}$  and  $\Lambda_c$ . This theory predicts  $\sigma_1(T_c) < \sigma_2(T_c)$ , in contrast to the previous theories which did not take account of the finite cutoff, and predicted  $\sigma_1(T_c) = \sigma_2(T_c)$  [15, 16]. Experimentally, the effect of the finite cutoff at  $T_c$  is clearly observed in Fig. 2(a). The experimental ratio  $\sigma_2(T_c)/\sigma_1(T_c)$  puts a constraint on the choices of  $\Lambda_{ab}$  and  $\Lambda_c$ . We have used the background free experimental value of  $\sigma_2(T_c)$  to evaluate the parameter  $\xi_{0c}$  in Eq. (2). We obtained  $\xi_{0c} = 0.05$  nm for the BSCCO-2212 sample. One should note that this does not correspond to the zero temperature coherence length along the *c*-axis, but the value obtained when the linear temperature dependence of the Ginzburg-Landau coefficient  $\alpha$  is extrapolated to zero temperature. Alternatively, one could say that  $\xi_{0c}^{-2}$  determines the slope of  $\alpha$  near  $T_c$ . The very small value for  $\xi_{0c}$  obtained here is not physically unacceptable. Similar results for  $\xi_{0c}$  were obtained also from *dc* conductivity measurements [17].

The temperature dependence in both, the prefactor and the  $\mathcal{S}$ -functions in Eq. (2), originates from  $\xi(T)/\xi_0$ . We have used the experimental values of  $\sigma_2(T)$  to solve for  $\xi(T)/\xi_0$  in Eq. (2). The results are shown in Fig. 2(b). One observes that in the BSCCO-2212 sample, for temperatures within 0.7K interval above  $T_c$ , the coherence length has a static critical exponent of  $\nu = 1$  (top dashed line in Fig. 2(b)). This narrow region is followed by a crossover to another critical regime extending from  $T_c + 8$ K to  $T_c + 35$ K. The static critical exponent in this region is close to  $\nu = 2/3$  (middle line in Fig. 2(b)) as expected for the 3D XY universality class. A closer inspection of this region on an expanded scale shown in the inset to Fig. 2(b), reveals that only the section at higher temperatures (from  $T_c + 18$ K to  $T_c + 35$ K) has exactly  $\nu = 2/3$ . At temperatures from  $T_c + 8$ K to  $T_c + 15$ K one can identify a straight line with a slope slightly higher than  $2/3$ . This could be either an additional critical state with  $\nu \gtrsim 2/3$ , or a perturbation of  $2/3$  slope caused by the tails of the neighbouring crossovers. Beyond  $T_c + 35$ K one observes a deviation from the 3D XY critical regime, probably marking the crossover to

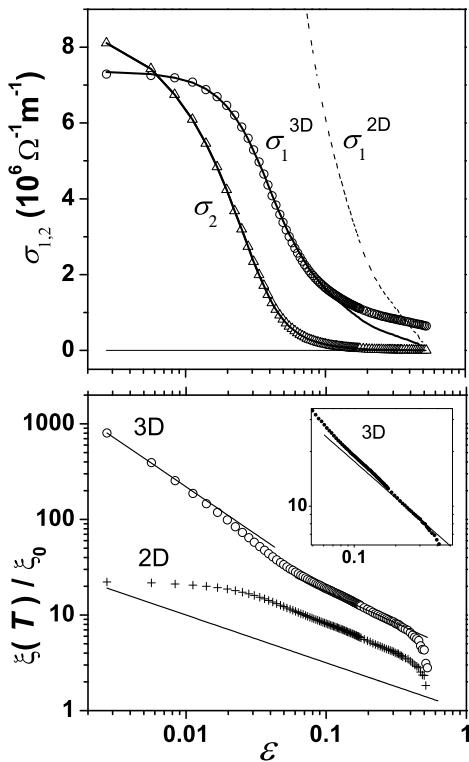


FIG. 2: (a) Temperature dependences of the total measured real (○) and imaginary part (△) of the complex conductivity above  $T_c$  in BSCCO-2212 thin film. The full and dashed lines are the results of the 3D and 2D calculations, respectively, as explained in the text. (b) The normalized coherence length extracted from the experimental data of  $\sigma_2$  in (a) by means of the 3D (○) and 2D (+) theoretical expressions. The lines show the slopes  $\nu = 1$  and  $\nu = 2/3$  for the two critical regimes, and the Gaussian limit  $1/\sqrt{\epsilon}$ . The inset shows 3D result on an enlarged scale.

the Gaussian regime with the critical exponent  $\nu = 1/2$  (bottom line in Fig. 2(b)). The dramatic drop seen in the last few points at  $\epsilon > 0.5$  can be interpreted in terms of the energy cutoff in the fluctuation spectrum [18, 19]. The extraction of the coherence length was based on the imaginary part of the  $ac$  fluctuation conductivity  $\sigma_2$  which certainly originates only from the superconducting fluctuations, i. e. it has no contribution from the normal electrons. We may now check the consistency of the analysis on the real part  $\sigma_1$ . Using the values of  $\xi(T)/\xi_0$  from Fig. 2(b), we calculate the corresponding values of  $\sigma_1$  from Eq. (2). The result is plotted as the full line in Fig. 2(a). One observes an excellent agreement between the calculated and the total measured real conductivity from  $T_c$  up to  $T_c + 8K$ . Beyond this region, the calculated values of  $\sigma_1$  fall below the total experimental  $\sigma_1^{tot}$ . It appears that in the first critical regime near  $T_c$ , and in the crossover to the second critical regime,

all the electrons participate in the superconducting fluctuations so that the fluctuation conductivity equals the total observed conductivity. However, when the second critical regime is established a fraction of the electron system remains in the normal state and gives rise to a normal conductivity contribution. This normal conductivity contribution is seen in Fig. 2(a) as the difference between the total measured  $\sigma_1^{tot}$  (symbols) and the calculated fluctuation conductivity  $\sigma_1$  (full line). With increasing temperature, the normal fraction of the electrons grows resulting in an increase of the normal conductivity contribution. The phenomenon in which the normal conductivity is depressed when  $T_c$  is approached has been proposed to result from a decrease of the one-electron density of states at the Fermi level due to the superconducting fluctuations [20, 21, 22].

We have also analyzed related experimental data of the BSCCO-2212 sample using the 2D expression for the  $ac$  fluctuation conductivity [14]. It contains the effective layer thickness as the parameter which we have set to 1.5 nm. The corresponding values of  $\xi(T)/\xi_0$  are also shown in Fig. 2(b). When using the 2D expression, a saturation of the coherence length is reached when  $T_c$  is approached, which is a completely unphysical result. Furthermore, when these values of  $\xi(T)/\xi_0$  and the 2D expression are used to calculate  $\sigma_1$ , one finds gross disagreement with the experimental data (dashed line in Fig. 2(a)). This analysis proves that BSCCO-2212 does not behave as a 2D system over the temperature range investigated here. Moreover, the Gaussian prediction  $\xi(T)/\xi_0 = 1/\sqrt{\epsilon}$  is incompatible with the experimentally observed values of  $\xi(T)/\xi_0$  which are much larger due to the critical fluctuations. Using the value  $\xi_{0c} = 0.05$  nm determined above, one finds  $\xi_c(T) > s/2$ , where  $s$  is the separation of the layers, up to the end of the critical regime with  $\nu = 2/3$ . Hence, the condition for 3D to 2D crossover is not reached and the critical state remains 3D XY. Only beyond this temperature range, where one observes a drop in the value of  $\xi_c(T)$ , one may expect the crossover to a 2D behavior with the Gaussian fluctuations. Unfortunately our signal to noise ratio does not allow a detailed analysis of this high temperature region.

Fig. 3 shows comprehensively the temperature dependences of the normalized coherence lengths in YBCO, BSCCO-2212, and BSCCO-2223 films. One observes readily that the appearance of multiple critical regimes of the superconducting fluctuations is a general feature in high- $T_c$  layered superconductors. The anisotropy of the system affects the temperature ranges of the critical states. The more anisotropic superconductors have their critical regimes extended to higher temperatures. BSCCO-2223 exhibits the first critical state with  $\nu = 1$  up to  $T_c + 1.4K$ , which is considerably more extended than found above in BSCCO-2212. The distinction between the second and the third critical regimes is more pronounced in BSCCO-2223. The third critical regime

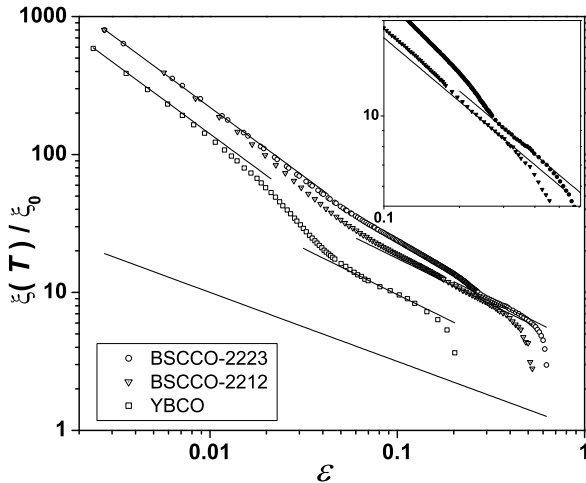


FIG. 3: Comparative presentation of the normalized coherence lengths in high- $T_c$  superconductors YBCO, BSCCO-2212, and BSCCO-2223 with various degrees of anisotropy.

(from  $T_c + 25\text{K}$  to  $T_c + 50\text{K}$ ) has exactly  $\nu = 2/3$ , while for the second critical regime (from  $T_c + 7\text{K}$  to  $T_c + 18\text{K}$ ) one could accept the same scenario as discussed in the case of BSCCO-2212.

YBCO is the least anisotropic material of the three superconductors studied here. We observe in Fig. 3 that it also develops the critical state with  $\nu = 1$ , but very close to  $T_c$ . The values of the reduced coherence length  $\xi(T)/\xi_0$  are much lower than in the BSCCO superconductors. It appears that in YBCO the second and third critical states merge into a single one which is squeezed into a much narrower temperature range from  $T_c + 4\text{K}$  to  $T_c + 10\text{K}$ . This finding is in agreement with the combined analysis of the  $dc$  conductivity, specific heat, and susceptibility measurements in YBCO single crystals [23]. Beyond  $T_c + 10\text{K}$  the reduced coherence length in YBCO shows a drop towards the Gaussian value  $1/\sqrt{\epsilon}$ . With such low values of  $\xi(T)/\xi_0$  the  $ac$  fluctuation conductivity becomes so small that our signal to noise ratio precludes a further analysis.

In conclusion, we have determined for the first time the absolute values of the normalized coherence length  $\xi(T)/\xi_0$  above  $T_c$  in high- $T_c$  superconductors. Our results show in detail how the fluctuations of the order parameter develop in YBCO, BSCCO-2212, and BSCCO-2223 systems with different degrees of anisotropy. In the vicinity of  $T_c$ , one finds a hitherto unobserved critical regime with the static critical exponent  $\nu = 1$ . At higher temperatures one observes in BSCCO samples a critical regime having  $\nu = 2/3$  as required in 3D XY universality class, while in the preceding intermediate temperature re-

gion the critical exponent could not be established with certainty due to the extended tails of the crossover regions. In YBCO the intermediate region is not resolved but seems to be merged into a single critical state with approximately  $\nu = 2/3$ , which is squeezed to a temperature range closer to  $T_c$ . The possibility of a 2D behavior in the critical regimes is disproved by the present analysis. The absolute values of the coherence length along the  $c$ -axis remain, throughout all the critical regimes, large enough ( $\xi_{0c}(T) > s/2$ ) to preserve the 3D nature of the fluctuations. The expected crossover to a 2D behavior could possibly occur in the Gaussian regime at even higher temperatures.

The authors acknowledge the preparation of the BSCCO-2223 thin film to Dr. A. Attenberger, and V. Rădulescu for the help in the development of the required software.

- 
- \* present address: D.-N. Peligrad: Philips Research Laboratories, Weisshausstrasse 2, D-52066, Aachen, Germany; B. Nebendahl: Agilent Technologies Deutschland GmbH, Herrenberger Str. 130, D-71034, Böblingen, Germany  
 Ⓜ Electronic address: dragos.peligrad@philips.com; m.mehring@physik.uni-stuttgart.de; adulcic@phy.hr
- [1] D. S. Fisher, M. P. A. Fisher, and D. A. Huse, Phys. Rev. **B43**, 130 (1991).
  - [2] S. Kamal et al., Phys. Rev. Lett. **73**, 1845 (1994).
  - [3] S. M. Anlage et al. Phys. Rev. **B53**, 2792 (1996).
  - [4] M. B. Salamon et al. Phys. Rev. **B47**, 5520 (1993).
  - [5] N. Overend, M. A. Howson, and I. D. Lawrie, Phys. Rev. Lett. **72**, 3238 (1994).
  - [6] R. Menegotto Costa et al., Phys. Rev. **B56**, 10836 (1997).
  - [7] S. H. Han, Yu. Eltsev, and Ö. Rapp, Phys. Rev. **B57**, 7510 (1998).
  - [8] S. H. Han, Yu. Eltsev, and Ö. Rapp, Phys. Rev. **B61**, 11776 (2000).
  - [9] V. Pasler et al., Phys. Rev. Lett. **81**, 1094 (1998).
  - [10] K. D. Osborn et al., cond. mat. 0204417, unpublished.
  - [11] B. Nebendahl et al., Rev. Sci. Instr. **72**, 1876 (2001).
  - [12] D.-N. Peligrad et al., Phys. Rev. B **64**, 224504 (2001).
  - [13] J. R. Waldram et al., Phys. Rev. **B59**, 1528 (1999).
  - [14] D.-N. Peligrad, M. Mehring, and A. Dulčić, submitted to Phys. Rev. B (2002), cond. mat. 0207748.
  - [15] H. Schmidt, Z. Phys. **216**, 336 (1968).
  - [16] A. T. Dorsey, Phys. Rev. **B43**, 7575 (1991).
  - [17] R. Hopfengärtner, B. Hensel, and G. Saemann-Ischenko, Phys. Rev. **B44**, 741 (1991).
  - [18] C. Carballeira et al., Phys. Rev. **B63**, 144515 (2001).
  - [19] J. Viña et al., Phys. Rev. **B65**, 212509 (2002).
  - [20] E. Abrahams, M. Redi. and J. W. F. Woo, Phys. Rev. **B1**, 208 (1970).
  - [21] C. DiCastro et al., Phys. Rev. **B42**, 10211 (1990).
  - [22] A. A. Varlamov et al., Adv. Phys. **48**, 655 (1999).
  - [23] M. V. Ramallo and F. Vidal, Phys. Rev. **B59**, 4475 (1999).